

Available online at www.sciencedirect.com



polymer

Polymer 44 (2003) 8053-8059

www.elsevier.com/locate/polymer

Morphological study of melt-crystallized poly(ethylene terephthalate): B. Thin films

H.G. Haubruge*, R. Daussin, A.M. Jonas, R. Legras

Laboratoire de Physique et de Chimie des Hauts Polymères, Université catholique de Louvain, Croix du Sud 1, B-1348 Louvain-la-Neuve, Belgium Received 10 February 2003; received in revised form 31 August 2003; accepted 14 October 2003

Abstract

Thin spin-casted films of poly(ethylene terephthalate), isothermally crystallized from the melt, were studied by transmission electron microscopy. An amorphous substrate was used to get rid of unwanted nucleating influences. The lamellar scale information gained by this technique agrees well with results obtained on bulk samples despite important differences in morphology at the spherulitic scale. Starting from thin films of constant thickness, crystallization involves the migration of the polymer to the growing spherulites, resulting in the formation of polymer-depleted interspherulitic gaps. Isolated and stacked lamellae growing on top of terrace-like flat-on crystals are also noticed, allowing the direct observation of the crystalline-amorphous interphase.

© 2003 Elsevier Ltd. All rights reserved.

Keywords: Polyethylene terephthalate; lamellar morphology; Spherulitic growth

1. Introduction

Many studies have been devoted to the effect of confinement of polymer chains in thin films, as contrasted from the bulk behavior of the polymer. Some of these effects may arise from the spin-casting process itself, which is the usual mean for obtaining thin film samples, but others were demonstrated for thermally relaxed films. Some of these effects hold true for homo- or copolymers indifferently, whether they are crystallizable or not.

The glass transition temperature $(T_{\rm g})$ of polystyrene and other polymers, for instance, decreases with thickness for unsupported films, and is lower than in bulk samples. In such free standing films, a complex influence of molecular weight is also apparent in sufficiently thin films, were chains confinement may appear [1]. The frequent decrease in $T_{\rm g}$ is usually linked to an increased mobility of the polymer chains near the free surface, although the underlying explanation is still the subject of much discussion. For supported films, however, strong interactions with the substrate may lead to a higher effective $T_{\rm g}$, even above the one in the bulk.

Confinement effects were also evidenced for crystal-

lizable macromolecules either in crystalline/amorphous block copolymer systems (see for instance Ref. [2] and references therein), or in thin films of homopolymers annealed from room temperature. The crystallization rate of the polymer in thin films was compared to the one in the bulk: for annealed 150 nm-thick poly(ethylene terephthalate (PET) films, e.g. the higher surface mobility leads to a higher surface crystallization rate than in the bulk [3]. This crystallization occurring from the surface was also highlighted in recent works on similar [4] or much thicker (a few microns) [5,6] PET samples. In other polymer systems and for very thin films, on the order of a few tens of nanometers, it was nevertheless shown that crystallization may be impaired by the difficulty to reach the critical nucleus size required in the first stages of crystal growth [7]. In such cases, a substantial decrease of the crystallization rate is observed. A similar phenomenon is probably at play in intercalated compounds [8], where it might, however, be partly compensated by a nucleation mechanism for some cases of favorable polymer/substrate interactions.

The film thickness also influences the crystal growth and the final semi-crystalline morphology. With decreasing thickness (from the micrometer scale to about 100 nm), one observes a transition from flattened polygonal spherulites to mostly edge-on lamellar sheaves [9–12] or flat-on crystals [11,12]. Below a certain critical thickness, some chain

^{*} Corresponding author. Tel.: +32-104-733-91; fax: +32-104-515-93. *E-mail address:* haubruge@poly.ucl.ac.be (H.G. Haubruge).

alignment parallel to the substrate is also often noticed [13]. Many studies have focussed on ultrathin films (from a few nanometers to a few tens of nanometers). In such systems, diffusion-controlled crystal growth leads to characteristic branched crystal patterns [14–16]. In any case, the crystal growth rate may become strongly limited by decreasing film thickness, which has been ascribed to a reduced mobility of the chains on interactive substrates [11,12,17]. In this context, the substrate might exert some nucleation enhancement by both its roughness [7,10] and its composition [10]. Complicating further the picture is the role of substrate roughness [18] and possible dewetting [19] on the final morphology, which were both investigated.

Although previous works on PET essentially focussed on the cold-crystallization of annealed films, results on the morphology of PET thin films crystallized from the melt were so far very limited. Work by Sakai and co-workers [9, 20] mainly focussed on the flat-on terrace growth occurring on the edge of essentially two-dimensional PET spherulites. Therefore, the purpose of the present paper is to gain more information on the crystalline lamellae present in such systems of intermediate thickness (i.e. sub-micron but not ultrathin). Image analysis is used to quantitatively characterize the lamellar morphology and to relate it to former observations in the bulk. Finally, specific morphological features of PET thin films are also discussed.

2. Experimental

Thin PET films were spin-casted on glass or carbon-coated mica sheets (evaporated C layer about 20 nm thick). PET (grade E47, ICI) was dissolved in hexafluoroisopropanol (HFIP, Acros) and the spincoater settings were 5000 rpm, 20,000 rpm/s and 60 s, at room temperature. In these conditions, reproducible thicknesses are obtained, as checked with a Jobin Yvon ellipsometer for samples deposited on silicon wafers. For the present work, PET concentrations of 25, 50 and 75 g/l were used, corresponding to film thicknesses of about 125, 250 and 375 nm, respectively.

These films were dried under vacuum, protected by a glass cover, then melted for 5 min at 280 °C in a Mettler Toledo FP82HT hot-stage, under an argon flow. A 20 °C/min cooling ramp brought them to the isothermal crystallization temperature, with a 30 min duration except at 230 °C where samples were left for 60 min to ensure complete crystallization.

Glass-supported thin films were observed by transmission with an Olympus AX70 optical microscope. Atomic force microscopy (AFM) analyses were realized under ambient conditions in intermittent-contact mode on a PicoSPM (Molecular Imaging), equipped with force modulation cantilevers with free resonance frequencies in the 55–65 kHz range, and controlled with a Nanoscope III electronics (Digital Instruments).

For transmission electron microscopy (TEM) observations, mica-supported samples were floated off water. These thin films, backed with their carbon layer, were retrieved on copper TEM grids and stained by ruthenium tetroxide according to a previously described method [21]. TEM micrographs were obtained with a Philips EM 301 operating at 80 kV. Image analysis was performed with Wavemetrics Igor Pro and custom procedures, including Gaussian filters used for image flattening.

3. Results and discussion

3.1. Influence of substrate and film thickness

One can speculate that in most crystallization studies, the substrate surfaces or the impurities they carry can act as nuclei for the molten polymer. In thin films, optical microscopy of spin-casted PET on freshly cleaved mica reveals specific patterns indicative of an epitaxial crystal growth. For these reasons, all experiments in this work were conducted on substrates characterized by a sufficient lack of surface order, namely glass or carbon-coated mica sheets.

Glass and carbon-coated mica surfaces are also flat enough and yet randomly rugous so as to avoid topological effects like graphoepitaxy. Nevertheless, solvent- and even spin-casting techniques do not prevent some local variations of the polymer film thickness. Fig. 1 gives an example of such variations in topography and show the tremendous differences in the spherulitic size that they may bring. Care is thus needed in the selection of zones with a polymer thickness, which is constant on the scale of the image size for spherulites characterization.

3.2. Influence of crystallization temperature

Annealed from the glass at 150 °C for 12 h, a spin-casted PET film remains continuous and apparently homogeneous on the micrometer scale. No spherulitic zones nor significative thickness variations are indeed observed by TEM on such RuO₄ stained samples. Lamellae-like structures with a long period around 9 nm and less seem to exist, but their very small lateral extension combined to

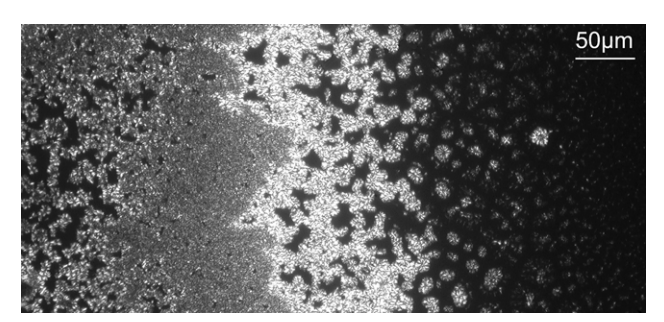


Fig. 1. Solvent-casted PET film isothermally crystallized from the melt at 200 °C. Optical micrograph taken at the border of a hole in the film, on the right. Evolution of spherulitic size with the sample thickness is observed.

the high-frequency noise of the surrounding environment makes it very difficult to quantitatively characterize such samples under direct observation by the TEM technique.

On the contrary, upon crystallization from the melt, large spherulitic structures become visible. Under some conditions, acicular structures may also appear, as described earlier [22]). These structures can be considered as immature spherulites, stopped in a early stage of growth by their neighbors, due to a dense nucleation.

In the bulk, increasing crystallization temperatures typically produce larger spherulites. In a general case, spherulitic growth in thin films is, however, limited by the availability of molten material due to the restricted geometry. A vertical expansion is thus taking place, where growing crystals are fed by diffusion of the neighboring

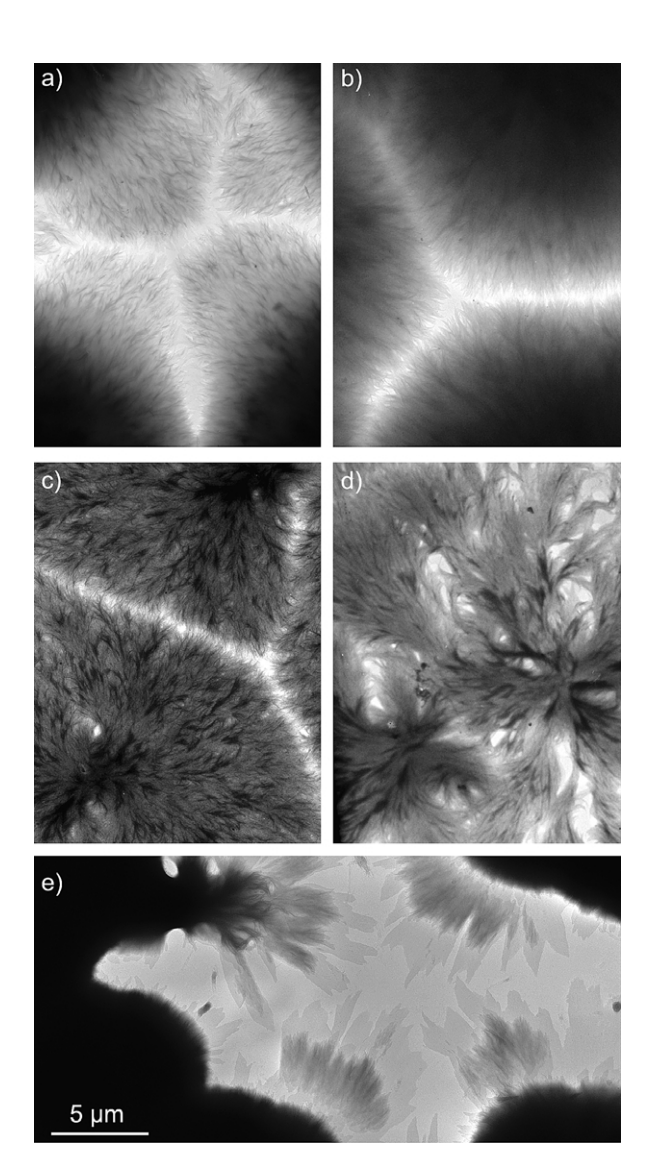


Fig. 2. TEM micrographs of stained PET thin films crystallized from the melt, showing the distinct spherulitic morphology. The respective spin-casted concentration and crystallization temperature were (a) 50 g/l, 200 °C, (b) 50 g/l, 230 °C, (c) 25 g/l, 220 °C, (d) 25 g/l, 230 °C and (e) 75 g/l, 220 °C. All figures are shown at the same magnification.

liquid polymer. Fig. 2 shows TEM micrographs emphasizing the spherulitic boundaries.

As spherulites are competing for the same molten material, some polymer depletion may occur in between. To a lesser extent, this also applies to lamellar fibrils and individual crystals. This is similar to the structures observed for HDPE in some circumstances, where fibrils are seen growing out of crystalline cores, "consuming most of the material and leaving a thin layer of disordered lamellae or uncovered substrate in between" [10]. In the extreme case of ultrathin films, a depletion zone separating flat-on crystals from the surrounding amorphous material, with a depth roughly proportional to the crystal thickness, has also been described [15]. The thickness gradient resulting from the protrusion of crystals from the surrounding melt is responsible for morphological instabilities [15]. The exact morphology of the film after crystallization is thus thought to be the result of a balance between crystallization and diffusion kinetics, both depending on the crystallization temperature, and possibly on the film thickness as well.

The contrast of spherulites in TEM therefore arises from their own thickness, even without staining. AFM measurements furthermore indicate that, starting from a 250 nmthick film, crystallization at 230 °C for 1 h may yield polymer peaks at 700 nm above the substrate, while spherulites borders are completely depleted. Fig. 2(e) displays an extreme example of this behavior, where very thick spherulites are surrounded by large gaps, mostly free of polymer except for characteristic flat-on crystals and lamellar overgrowths, which are discussed later. It is obvious that samples of such thickness cannot reveal their inner lamellar morphology by TEM. However, adequate contrasting of the spherulites fringes allows the observation of individual or stacked lamellae. Decreasing film thickness progressively allows observation of lamellae on larger border zones (Fig. 2(a) and (b)) or on the whole spherulite surface (Fig. 2(c) and (d)). Near the spherulites core, however, the strong thickness variations makes it always difficult to focus on many lamellar crystals simultaneously. For these reasons, the majority of long period measurements presented below were obtained on the fringes of spherulites on thin films spin-casted from a 50 g/l solution. Nevertheless, measurements on samples of various thickness are in good agreement with these values.

3.3. Lamellar crystals and order-disorder interphases

A typical TEM micrograph of PET lamellae developed in a thin film is given in Fig. 3. Lamellae may clearly be involved in multiple stacks along their growth path. Some of them even seem to bridge lamellar stacks between neighboring spherulites, although the thinness of the interspherulitic zones makes it hard to follow unique lamellae there (not shown on the figure). Other lamellae display a very high curvature, although no external constraints are applied during quiescent crystallization.



Fig. 3. Individual and stacked lamellae in the border area of a spherulite, grown from a PET thin film crystallized for 1 h at 230 °C. Some lamellae are seen taking part in multiple stacks.

The long period of stacked lamellae can be measured from the one-dimensional power spectral density (PSD) of an arbitrary micrograph if the population of stacks is dense enough [23]. If not, the large polymer-depleted gaps between lamellae tend to shift the long spacing obtained from the PSD towards artificially high values. In this case, one must rely on the average of manual measurements of profiles along the stacks cross-section. For this work, both methods were used when applicable, or only direct profiling, which can estimate a long period even for just a pair of aligned lamellae.

The resulting evolution of the semi-crystalline long period with the crystallization temperature (T_c) is displayed in Fig. 4, and compared to similar data points obtained for

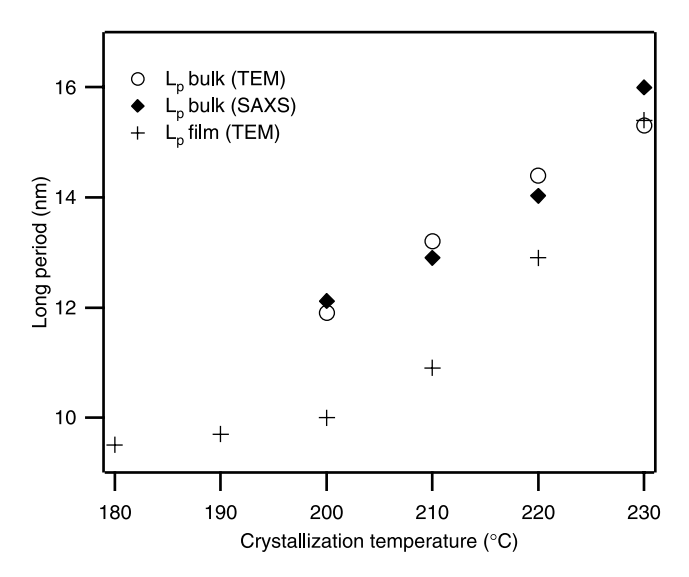


Fig. 4. Long period of PET as a function of the crystallization temperature, in the bulk and in thin films. Measurements are made from TEM micrographs of stained thin films or bulk sections, and by SAXS on bulk samples. The long period in thin films was evaluated by direct profiling of all samples, and also from the power spectral density of samples crystallized at 230 and 220 $^{\circ}$ C.

bulk samples [24]. Although the absolute values are diverging for decreasing $T_{\rm c}$, the general trend is the same. The observed discrepancies could come from an intrinsic difference in crystallization kinetics depending on the sample geometry, but they could also be linked to differences in the cooling conditions (bulk samples are crystallized in a differential scanning calorimetry instrument while thin films are crystallized on a hot-stage). On the other hand, the $L_{\rm p}$ plateau that is progressively reached below 200 °C is probably due to an insufficient cooling rate, allowing partial crystallization at higher temperatures.

Following the evolution of the lamellar thickness (l_c) as a function of crystallization temperature from TEM micrographs is a much more difficult task. Whereas L_p can be easily measured whenever regularly spaced lamellae are present (from peak to peak in grey level intensities along a line profile), l_c evaluation requires a fairly good baseline and peak definition to evaluate the mid-height width. Due to the high-frequency nodular noise present on all our TEM observations of PET, these requirements are not easily fulfilled here. Although no statistically meaningful values can thus be given, it can still be estimated from the micrographs that the lamellar thickness is on the order of half the long period at any T_c . Slight variations of thickness may also be noticed along some lamellae. This supports the idea that the distribution of lamellar thickness also results from a continuous variation of thickness along the lamellar length, as shown recently by HRTEM on poly(3-oxotrimethylene) [25], and not only from interlamellar variations, nor even from the existence of distinct populations of lamellae.

Since melt-crystallized PET thin films often present isolated lamellae, there exists an opportunity of directly measuring the order-disorder interphase in these systems. In such regions, the very limited sample thickness results in the contrast arising essentially from differential staining, as opposed to topography. Fig. 5 displays the average crosssectional profile obtained for such an individual lamella. On both sides of the crystal core, which appears in a whitish grey in the center of Fig. 5, darker stripes indicate the presence of stained amorphous zones, progressively dissipating as one draws further away from the crystal to enter in the polymer-depleted empty background (in white). From the profile of grey levels across the lamella and its surroundings, one can provide estimations for the lamellar core thickness, and the thickness of the amorphous regions bordering the lamella: these amounts to 6 and 9 nm, respectively. Although the measured extent of these regions depends on the absolute grey level intensity observed for the background, the key information here is the existence of non-crystalline stainable regions surrounding a lone polymer crystal, which we attribute to the crystal/amorphous interphase regions. This indicates that for a semi-stiff polymer like PET, the creation of lamellae from the melt, implies a dissipation of order over a distance range at least comparable to the width of amorphous zones inside stacks

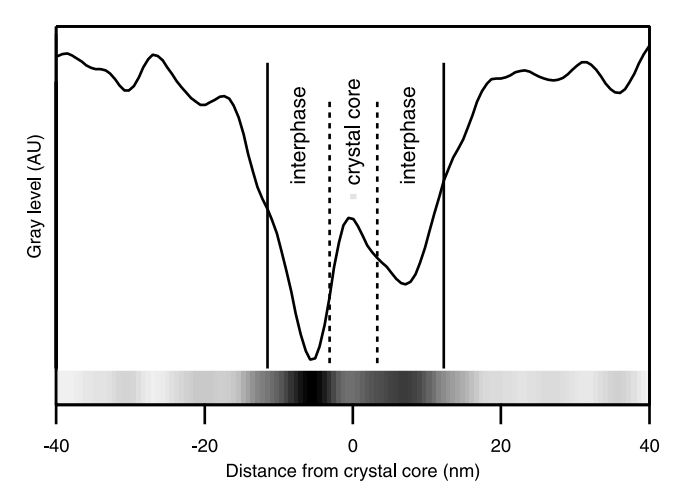


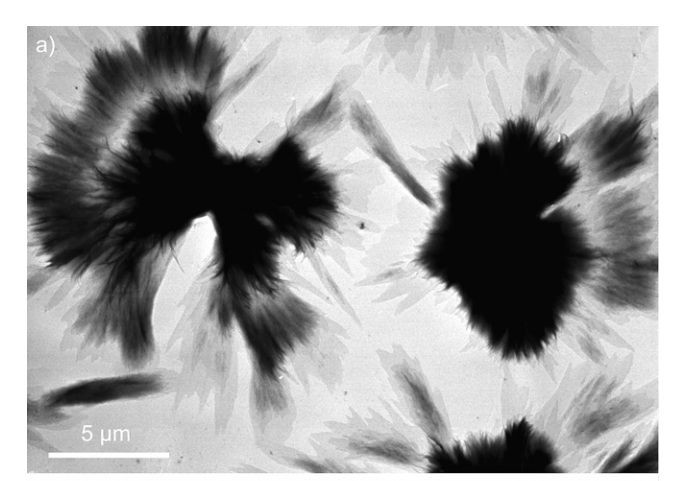
Fig. 5. Grey level intensity profile along the cross-section of an isolated lamella, grown at 230 °C. Successive profiles were averaged from the sampled area, shown in Fig. 6(c) and corresponding to about 100 nm of lamellar length. Dashed lines delimitate the crystalline core, while solid lines indicate the extent of the adjacent amorphous regions. These boundaries are conventionally set at mid-height between stained (dark) and non-stained (white) regions [26].

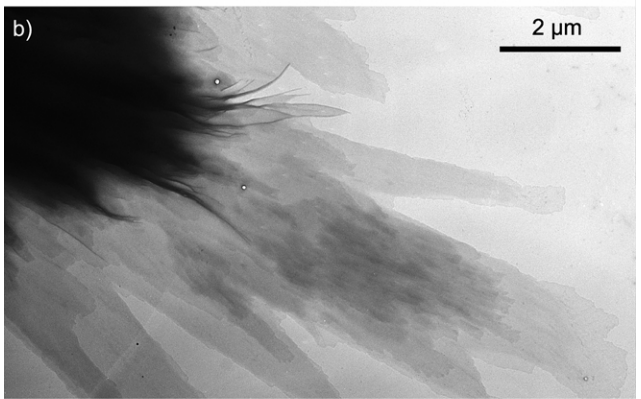
of lamellae. These results confirm, for pure PET, previous observations of crystal boundaries obtained for PET/PEI blends [26].

3.4. Flat-on crystals and propagation of crystal growth

Another specific feature of melt-crystallized PET thin films is the presence of flat-on crystals seemingly radiating from the edges of spherulites (see Fig. 6(a)). While TEM observations reveal a quenched state after complete crystallization, studies using in situ confocal scanning laser microscope show that these flat-on crystals appear only after the growth stage of the spherulites [20]. This peculiar morphology was tentatively attributed to a tip-splitting growth occurring from a very thin molten layer, after most of the amorphous material has been depleted by the growing spherulite [9,20]. It should be noted that these crystals are also observed in less extreme cases of depletion, although they are then protruding a few hundreds of nanometers only (see for instance the borders of spherulites in Fig. 2(a)).

Despite the absence of shadowing on TEM samples, thickness variations alone sometimes allow to distinguish several superposed layers of flat-on crystals, probably originating from spiral dislocations [9]. By comparison with Fig. 6(a), Fig. 6(b) clearly shows that such layers, anyhow they become fragmented, should not be confused with lamellar overgrowth. Indeed, distinct edge-on lamellae (or fibrils) are clearly seen radiating outside the spherulite. Stacked flat-on layers might, however, favor their growth, as these lamellae are seemingly following edges or ridges of the underlying crystals. Fig. 6(c) shows this behavior at higher magnification, in a very thin region where a small flat-on 'finger' is bordered, and partly covered, by stacks of a few lamellae or by isolated ones.





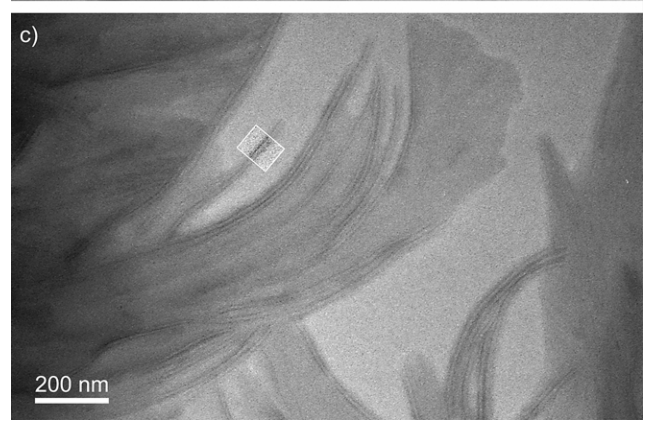


Fig. 6. Structures appearing on TEM micrographs of PET melt-crystallized at $230\,^{\circ}\text{C}$: (a) spherulites, (b) flat-on crystals and (c) edge-on lamellae. In (a) and (b), contrast due to thickness is dominant, while in (c) it also arises from the preferential staining of the amorphous phase. The highlighted rectangular area in (c) corresponds to the zone where the average line profile of Fig. 5 was computed.

The question then arises of how the molten material at the origin of these overgrowths is able to diffuse on top of the flat-on crystals, if themselves already formed from a very thin amorphous layer. Nevertheless, other observations highlight the role of flat-on crystals and/or overgrown lamellae in the propagation of crystal growth to non-depleted zones. Fig. 7(a) clearly shows well developed lamellar fibrils radiating from the spherulite on top of the flat-on crystals. On thicker films, the depletion zone at the

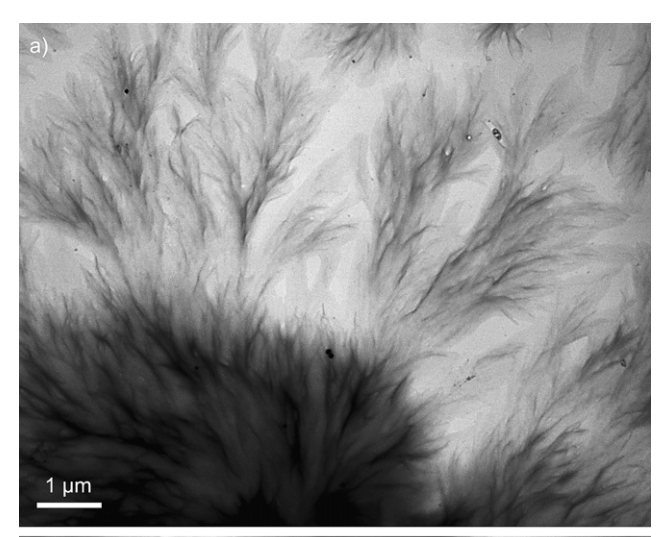




Fig. 7. Propagation of waves of crystal growth along flat-on crystals and/or overgrown lamellae: crystallization from the melt at (a) 180 $^{\circ}$ C and (b) 230 $^{\circ}$ C.

edge of the spherulite is even more apparent. Some lamellae are crossing it, always on top of a flat-on crystal, and could initiate more lamellar overgrowth as soon as new source of molten material is reached. Two such successive waves of crystal growth are depicted in Fig. 7(b).

4. Conclusion

Spherulitic growth on thin (around 250 nm) PET films is governed by the restricted geometry of these systems. The balance between crystallization kinetics and diffusion of molten material is responsible for a structure characterized by spherulites of decreasing thickness from center to periphery, surrounded by completely polymer-depleted regions. At the end of the crystallization process, the central area of the spherulites is thus considerably higher than the initial thickness of the starting film.

Individual lamellar crystals and stacks of lamellae are observed in sufficiently thin regions. The long period of stacks, measured by direct profiling on TEM micrographs, displays the same trends as a function of the crystallization temperature as results obtained for bulk samples. The crystalline thickness of lamellae is much more difficult to quantify, but is on the order of half the long period.

The direct observation of the order—disorder interphases around a crystalline lamella also casts some light on the internal structure of stacks of lamellae. Since even individual lamellae are always surrounded by non-crystalline stainable material, what is classically considered as interlamellar amorphous regions might actually be seen as regions of dissipating order, in agreement with previous work [26].

Finally, it is observed that flat-on crystals characteristic of PET thin films are in complex interactions with edge-on lamellar structures. Although these crystals were described as originating from diffusion of polymer material from a thin melt layer [20], present observations rise questions about the formation of lamellar overgrowths on these underlying crystals. The role of both flat-on crystals and edge-on lamellae in the propagation of a second wave of crystal growth in areas still rich in polymer may also be pointed out. An interesting perspective would thus be to closely monitor the appearance and morphological evolution of these structures in real-time, for instance by AFM.

Acknowledgements

This work was financially supported by the National Fund for Scientific Research (FNRS).

References

- Forrest JA, Dalnoki-Veress K. Adv Colloid Interface Sci 2001;94: 167.
- [2] Reiter G, Castelein G, Sommer JU, Röttele A, Thurn-Albrecht T. Phys Rev Lett 2001;87(22):226101.
- [3] Hayes NW, Beamson G, Clark DT, Law DSL, Raval R. Surf Interface Anal 1996;24:723.
- [4] Durell M, Macdonald JE, Trolley D, Wehrum A, Jukes PC, Jones RAL, Walker CJ, Brown S. Europhys Lett 2002;58(6):844.
- [5] De Cupere VM, Rouxhet PG. Polymer 2002;43:5571.
- [6] Damman P, Zolotukhin MG, Villers D, Geskin VM, Lazzaroni R. Macromolecules 2002;35:2.
- [7] Despotopoulou MM, Frank CW, Miller RD, Rabolt JF. Macromolecules 1996;29(18):5797.
- [8] Lincoln DM, Vaia RA, Wang ZG, Hsiao BS, Krishnamoorti R. Polymer 2001;42:9975.
- [9] Sakai Y, Imai M, Kaji K, Tsuji M. Macromolecules 1996;29:8830.
- [10] Mellbring O, Kihlman OS, Krozer A, Lausmaa J, Hjertberg T. Macromolecules 2001;34(21):7496.
- [11] Schönherr H, Frank CW. Macromolecules 2002;36(4):1188.
- [12] Schönherr H, Frank CW. Macromolecules 2002;36(4):1199.
- [13] Bartczak Z, Argon AS, Cohen RE, Kowalewski T. Polymer 1999; 40(9):2367.
- [14] Reiter G, Sommer JU. J Chem Phys 2000;112(9):4376.
- [15] Taguchi K, Miyaji H, Izumi K, Hoshino A, Miyamoto Y, Kokawa R. Polymer 2001;42:7443.
- [16] Zhang F, Liu J, Huang H, Du B, He T. Eur Phys J, E 2002;8(3):289.

- [17] Dalnoki-Veress K, Forrest JA, Massa MV, Pratt A, Williams A. J Polym Sci: Part B: Polym Phys 2001;39:2615.
- [18] Müller-Buschbaum P, Gutmann JS, Lorenz-Haas C, Mahltig B, Stamm M, Petry W. Macromolecules 2001;34(21):7463.
- [19] Kressler J, Wang C. Langmuir 1997;13(16):4407.
- [20] Sakai Y, Imai M, Kaji K, Tsuji M. J Crystallogr G 1999;203:244.
- [21] Haubruge HG, Jonas AM, Legras R. Polymer 2003;44(11):3225.
- [22] Nedkov E, Mihailov M. Izvestiya po Khimiya 1979;12(3):403.
- [23] Haubruge HG, Gallez X, Nysten B, Jonas AM. J Appl Crystallogr 2003;36(4).
- [24] Haubruge HG, Jonas AM, Legras R. 2003; Macromolecules. submitted.
- [25] Fujita M, Tsuji M, Kohjiya S. Macromolecules 2001;34(22):7724.
- [26] Ivanov DA, Pop T, Yoon DY, Jonas AM. Macromolecules 2002;35: 9813.